Energy Proceedings
Vol 59, 2025
ISSN 2004-2965

Long-term photovoltaic power generation prediction based on GNN-LightTS

Ke Yan[1]*, Jiazhen Zhang[1], Kangning Wu[1], Qianyu Yang[1], Ying Li[1]

1 College of Mechanical and Vehicle Engineering, Hunan University, Changsha, 410082, China

(*Corresponding Author: keyan@hnu.edu.cn)

ABSTRACT

Accurate prediction of photovoltaic power generation is crucial for the effective integration of renewable energy into the power grid, which is beneficial for real-time balance of the power grid and optimization of energy storage systems. However, due to the intermittency and volatility of photovoltaic power generation, achieving accurate photovoltaic prediction remains a challenge, especially for long-term photovoltaic prediction. This paper proposes a new method for long-term photovoltaic power generation prediction. This method innovatively combines graph neural network and LightTS model. Experiments were conducted using the proposed model on datasets from three photovoltaic power stations characterized by distinct terrain and climate conditions. The results show that our model surpasses all benchmark models in long-term forecasting and also achieves notable superiority in medium- and short-term predictions.

Keywords: Long-term photovoltaic power generation prediction, GNN, LightTS

NONMENCLATURE

Abbreviations	*Meaning*
GNN	Graph neural network
IEBlock	Information Exchange Block
MSE	Mean squared error
MAE	Mean absolute error

1. INTRODUCTION

With the increasing environmental pollution caused by traditional fossil energy and the continuous growth of energy demand, the demand for renewable energy is on the rise. Among renewable energy sources, solar energy has become a common choice due to its easy accessibility and huge potential energy[1]. Photovoltaic technology has received significant attention for generating clean and sustainable energy. However, photovoltaic power generation is often affected by weather and surrounding environment, causing fluctuations and intermittency, which poses considerable obstacles to integrating photovoltaic systems into the grid[2]. Accurate photovoltaic power generation prediction can enhance the stability and security of the grid, playing a crucial role in balancing the grid, ensuring automatic generation control, and maintaining the normal operation of the grid system[3]. While short-term photovoltaic power generation prediction has made significant progress, long-term photovoltaic prediction still faces significant challenges[4]. Compared to short-term photovoltaic prediction, long-term photovoltaic prediction can enable earlier planning to ensure the stable operation of the grid and avoid losses, greatly promoting the development of photovoltaic power generation.

With the development of big data and artificial intelligence, data-driven prediction methods and deep learning methods have become the mainstream of photovoltaic power generation prediction methods[5]. Particularly, models based on MLP not only have the characteristic of being lightweight but also achieve good results in solving long-term sequence prediction problems, with prediction accuracy even surpassing the variants of Transformer, thus receiving more attention. However, these methods rarely consider the covariates of the target variable. In fact, photovoltaic power generation data is often multivariate data. Effectively utilizing covariates for auxiliary prediction can achieve higher accuracy. Graph neural networks can well capture spatial dependencies. This paper attempts to use the LightTS[6] model combined with graph neural networks for long-term photovoltaic power generation prediction. The main contributions are as follows:

Multivariate interaction: Considering the influence of environmental variables on photovoltaic power generation, this paper innovatively uses graph neural networks to extract the complex relationships between the target variable and covariates, constructing a dynamic adjacency matrix, and conducting multivariate

This is a paper for the 11th Applied Energy Symposium: Low Carbon Cities & Urban Energy Systems (CUE2025), July 18-22, 2024, Kitakyushu, Japan.

information interaction through the dynamic adjacency matrix.

Long-term prediction: This paper uses the lightweight LightTS model for long-term photovoltaic power generation prediction. The LightTS model has two sampling methods: continuous sampling and interval sampling, which can efficiently capture the long-term and short-term patterns of long-term sequences, achieving high prediction accuracy while maintaining high efficiency.

2. RELATED WORKS

Existing photovoltaic prediction methods include physical, statistical, artificial intelligence, and hybrid methods. Physical methods establish mathematical models of photovoltaic power generation equipment, providing deterministic analytical solutions for photovoltaic prediction. Physical models use numerical weather forecasts or ground measurement devices and are calibrated for appropriate service facilities[7]. Statistical prediction involves extensive numerical model analysis based on statistical theory and requires domain knowledge datasets. However, statistical and physical models have been proven to be insufficiently effective, with lower accuracy in various important issues such as photovoltaic prediction and weather prediction. Artificial intelligence, particularly some advanced deep learning methods, can achieve accurate results and better generalization capabilities. Hybrid methods combine two or more methods to improve the performance of photovoltaic prediction[8]. In the case of using hybrid methods, the shortcomings in one method can be addressed by others, thereby improving the performance of photovoltaic prediction. However, hybrid methods face challenges of complex modeling and high computational costs, while deep learning techniques are more efficient for photovoltaic prediction.

3. MATERIAL AND METHODS

3.1 Dataset description

The data in this paper is sourced from the solar power station dataset collected by Chen[9] et al. using the SCADA system. The solar power stations are located in North China, Central China, and Northwest China, with different climates and geographical locations. The power generation capacity ranges from 30 megawatts to 200 megawatts. The data was sampled at a resolution of 15 minutes for 24 months. In this paper, three stations were selected for experiments. The data was processed for outliers and anomalies, and then divided into training, testing, and validation sets in a ratio of 7:2:1.

3.2 Proposed model

As illustrated in Fig. 1, the overall framework of the proposed model consists of two components. Firstly, a GNN framework aims to fuse target node's information with its neighbors' information. The data after variable interaction is input into LightTS model for photovoltaic generation prediction.

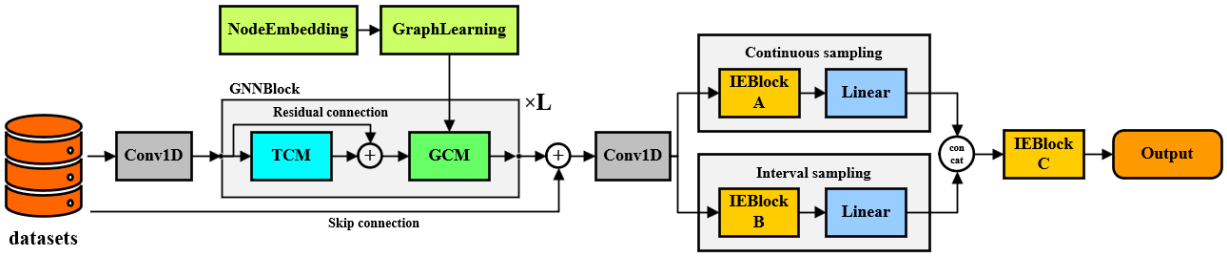

Fig. 1 The proposed model

GNN architecture adopted in this paper is MTGNN[10]. MTGNN is a graph neural network framework specifically designed for multivariate time series data. MTGNN mainly consists of a graph learning layer and a graph convolution module. The temporal convolution module simply applies a set of standard dilated 1D convolution filters to extract high-level temporal features.

The graph learning layer learns an adjacency matrix adaptively to capture the hidden relationship among time series data, the graph learning layer is specifically designed to extract unidirectional relationships, illustrated as follows:

$$E_1 = Embedding\left(nnodes, dim\right) \quad (1)$$

$$E_2 = Embed\left(nnodes, dim\right) \quad (2)$$

$$M_1 = \tanh\left(\alpha E_1 \theta_1\right) \quad (3)$$

$$M_2 = \tanh\left(\alpha E_2 \theta_2\right) \quad (4)$$

$$A = ReLU\left(\tanh\left(\alpha\left(M_1 M_2^{\,T} - M_2 M_1^{\,T}\right)\right)\right) \quad (5)$$

$$idx = argtopk\left(A\right) \quad (6)$$

where nnodes represents the number of variables and dim represent the number of dimensions. E1, E2 represents randomly initialized node embeddings, which are learnable during training, θ_1 and θ_2 are model parameters, α is a hyper-parameter for controlling the saturation rate of the activation function, and argtopk(·) returns the index of the top-k largest values of a vector.

The graph convolution module aims to fuse the target node's information of with its neighbors' nodes. The main component of this module consists of two mix-hop propagation layers to process inflow information and outflow information through each node separately. Given a graph adjacency matrix. The mix-hop propagation layer handle information over dependent nodes. The mix-hop propagation layers have two steps-information propagation step and the information selection step, The information propagation step is defined as follows:

$$H^{(k)} = \beta H_{in} + (1-\beta) A' H_{out} \tag{7}$$

where β is a hyper parameter, which controls the ratio of retaining the root node's original states. The information selection step is defined as follows:

$$H_{\text{out}} = \sum_{i=0}^{K} H^{(k)} W^{(k)} \tag{8}$$

where K is the depth of propagation, H_{in} represents the input hidden states outputted by the previous layer, H_{out} represents the output hidden states of the current layer.

We adopt LightTS model for PV power forecasting. LightTS based on MLP is a lightweight model. LightTS consists of two parts. The key components of these two parts are two sampling methods called continuous sampling and interval sampling, and three Information Exchange Blocks (IEBlock). The two sampling methods respectively focus on capturing the short-term local patterns and long-term global patterns. IEBLOCK is the basic building block for LightTS, the goal of an IEBlock is to leverage the information exchange along different dimensions.

IEBlock takes a 2D matrix of shape $H \times W$, where H is the temporal dimension and W is the channel dimension, and outputs another feature map of shape $F \times W$(F is the hyperparameter that corresponds to the output feature dimension). An IEBlock's process is illustrated as follows:

First, an MLP of $R^H \to R^{F'}$ is applied in each column. $Z = (z_{ij})_{H \times W}$ denotes the input 2D matrix, $z_{\cdot i} = (z_{1i}, z_{2i}, \cdots, z_{Hi})^T$ denotes the i-th column and $z_{j\cdot} = (z_{j1}, z_{j2}, \cdots, z_{jW})^T$ denotes the j-th row.

$$z^t_{\cdot i} = MLP(z_{\cdot i}) \tag{9}$$

Next, the temporal projection extracts features along the temporal dimension, an MLP of $R^W \to R^W$ is applied on each row:

$$z^c_{j\cdot} = MLP(z^t_{j\cdot}) \tag{10}$$

Finally, the channel projection exchanges information among different channels and keeps the input shape unchanged. An MLP of $R^{F'} \to R^F$ is applied on each column to map the feature dimension from F' to F:

$$z^o_{\cdot i} = MLP(z^c_{\cdot i}) \tag{11}$$

4. EXPERIMENT AND RESULTS

This paper conducts experiments using data collected from three photovoltaic sites and selects six new model algorithms as benchmark models for comparison.

4.1 Evaluation metrics

To compare the predictive performance among different models, we select two evaluation metrics: the mean squared error (MSE) and the mean absolute error (MAE), which are defined as follows:

$$MSE = \frac{1}{\mathrm{n}} \sum_{i=1}^{n} (x^i_{pred} - x^i_{true})^2 \tag{12}$$

$$MAE = \frac{1}{n} \sum_{i=1}^{n} \left| x^i_{pred} - x^i_{true} \right| \tag{13}$$

where x^i_{pred} is the predicted value of the model, and x^i_{true} is the corresponding true value.

4.2 Experiment results

This paper selects seven models, namely MTGNN, LightTS, DLinear[11], Transformer[12], Autoformer[13], Crossformer[14], and Informer[15], as benchmark models for long-term photovoltaic prediction and compares their prediction results with the proposed model to verify the effectiveness of the proposed model. The proposed model and benchmarks models gradually expand the horizon for single-step photovoltaic prediction, with the selected horizon being 96, 192, 384, and 768, and the input horizon 96. Each experiment is conducted ten times, and the average result is taken as the final experimental result. We highlight the best results in bold and use underlines to indicate the second-best prediction performance.

The experimental results of the three selected sites are shown in Tables 1, 2, and 3. When the Horizon is 96 and 192, Crossformer and MTGNN achieve better

prediction results than other benchmark models at sites 1 and 2, indicating that Crossformer and MTGNN have strong short-term prediction capabilities. At Horizon 384, Crossformer demonstrated better performance at sites 1 and 2. Notably, when the Horizon is 768**,** the prediction performance of the graph neural network MTGNN is generally better than that of other benchmark models. This might be because the covariate information extracted by the graph neural network is beneficial for long-term prediction. Overall, the proposed model consistently outperforms other models, and is particularly evident in the long - term prediction results, indicating that the graph neural network improves the prediction accuracy of LightTS and demonstrates superior performance in both short-term and long-term predictions.

Tabel 1. Prediction results of different methods of site 1

	Horizon96		Horizon192		Horizon384		Horizon768	
Methods	MSE	MAE	MSE	MAE	MSE	MAE	MSE	MAE
MTGNN	0.815	0.522	1.087	0.633	1.282	0.714	1.446	0.797
LightTS	0.855	0.542	1.086	0.647	1.330	0.729	1.563	0.803
DLinear	0.841	**0.491**	1.050	**0.579**	1.278	0.713	1.505	0.832
Transformer	0.917	0.612	1.405	0.766	1.515	0.855	1.606	0.865
Crossformer	0.829	0.515	1.046	0.638	1.267	0.743	1.502	0.820
Autoformer	1.397	0.812	1.375	0.785	1.578	0.862	1.709	0.903
Informer	1.356	0.799	1.515	0.877	1.763	0.947	1.953	0.999
GNN-LightTS	**0.793**	0.514	**1.011**	0.617	**1.207**	**0.698**	**1.423**	**0.767**

Tabel 2. Prediction results of different methods of site 2

	Horizon96		Horizon192		Horizon384		Horizon768	
Methods	MSE	MAE	MSE	MAE	MSE	MAE	MSE	MAE
MTGNN	0.870	0.425	0.853	0.455	0.989	0.537	1.009	0.514
LightTS	0.828	0.417	0.946	0.470	1.025	0.502	1.105	0.522
DLinear	0.848	0.406	0.954	0.450	1.048	**0.475**	1.092	0.491
Transformer	1.003	0.568	1.116	0.663	1.464	0.755	1.297	0.676
Crossformer	0.772	0.408	0.893	0.481	0.939	0.537	1.058	0.513
Autoformer	1.374	0.733	1.456	0.734	1.325	0.695	1.285	0.644
Informer	1.352	0.711	1.372	0.72	1.576	0.821	1.701	0.831
GNN-LightTS	**0.731**	**0.371**	**0.822**	**0.449**	**0.924**	0.522	**0.965**	**0.463**

Tabel 3. Prediction results of different methods of site 3

	Horizon96		Horizon192		Horizon384		Horizon768	
Methods	MSE	MAE	MSE	MAE	MSE	MAE	MSE	MAE
MTGNN	0.867	0.634	0.855	0.640	**1.017**	**0.703**	1.013	0.696
LightTS	0.904	0.663	1.015	0.709	1.094	0.741	1.156	0.762
Dlinear	0.835	0.644	0.966	0.700	1.037	0.731	1.128	0.765
Transfomer	0.759	**0.591**	0.892	0.656	1.119	0.716	1.054	0.714
Crossformer	0.765	0.603	1.103	0.633	1.326	0.704	1.493	0.776
Autoformer	1.038	0.766	1.244	0.846	1.066	0.792	1.271	0.865
Informer	1.312	0.834	1.395	0.885	1.676	0.968	1.823	1.037
GNN-LightTS	**0.744**	**0.602**	**0.814**	**0.623**	1.018	0.709	**0.981**	**0.685**

To further compare the prediction results of long-term photovoltaic power generation, we draw the histogram of the prediction results at the three sites when the Horizon is 768 to facilitate a more intuitive comparison of the prediction effects of all models. As shown in Fig. 2, The proposed model outperforms all benchmark models and achieves the best prediction effect at all sites, demonstrating good robustness. MTGNN comes second, and Crossformer performs better than other benchmark models at sites 1 and 2 but not as well as Transformer at site 3，This result may be related to the variation pattern of photovoltaic power generation at different sites.

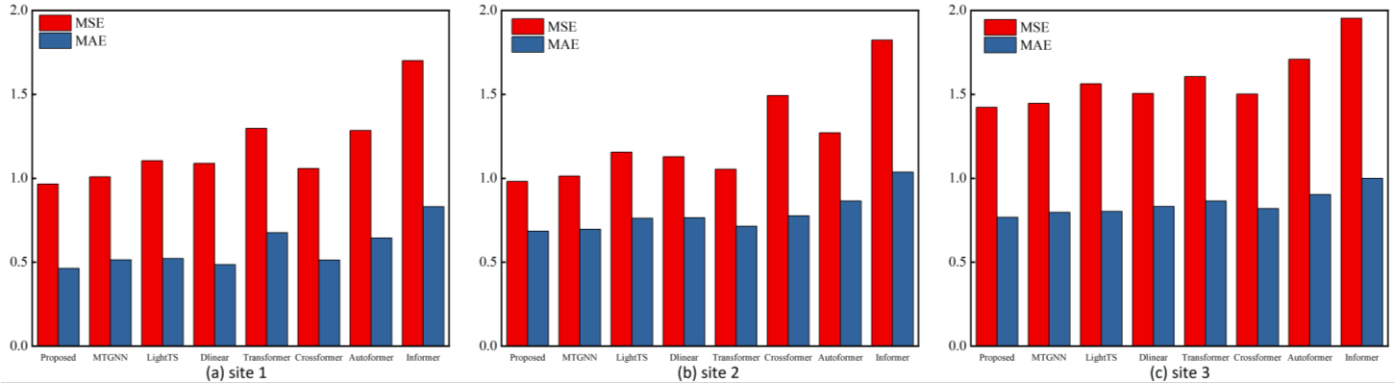

Fig. 2 MAE and MSE value

To further investigate the relationship between the model's predictive performance and the variation patterns of photovoltaic power generation, we have plotted the prediction curves of the models. To present the experimental results more clearly, we only selected the top five models with higher comprehensive rankings to compare their prediction effects on Horizon 768. Figures 3, 4 and 5 show the predicted curves of the models and the actual curves. Sites 1 and 2 exhibit relatively stable performance, while the photovoltaic power output at Site 3 varies drastically. This can be attributed to the more complex terrain and climatic conditions at Site 3, due to the influence of terrain and climate, the photovoltaic power generation at site3 fluctuates sharply, which leads to a decline in the prediction effect of the models.

The prediction curve of Transformer shows poor fitting at the troughs for Site 1 and Site 2, while its performance at the troughs of Site 3 is relatively better. This may be attributed to the Transformer model's heightened sensitivity to the highly volatile peaks at Site 3, which elevates the overall prediction curve and consequently compensates for its weaker performance in trough fitting.

In conclusion, though different terrains and climates can affect the prediction accuracy of the model and lead to unstable predictions, the proposed model (GNN-LightTS) always fits the actual values better than other methods in medium and long-term predictions and demonstrates superior prediction performance.

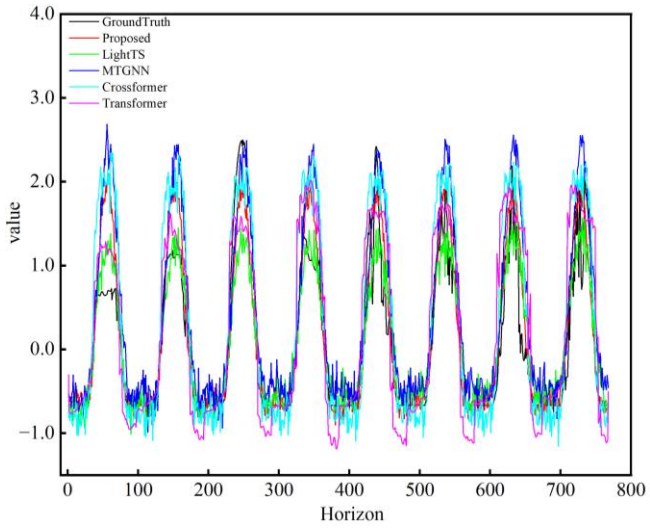

Fig. 3 prediction curves of site 1

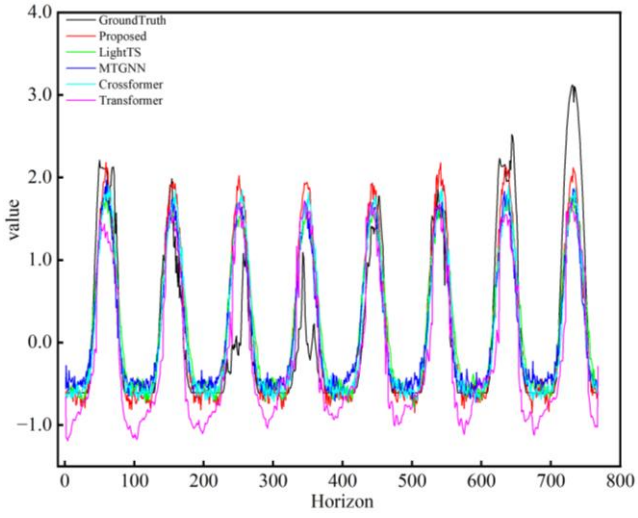

Fig. 4 prediction curves of site 2

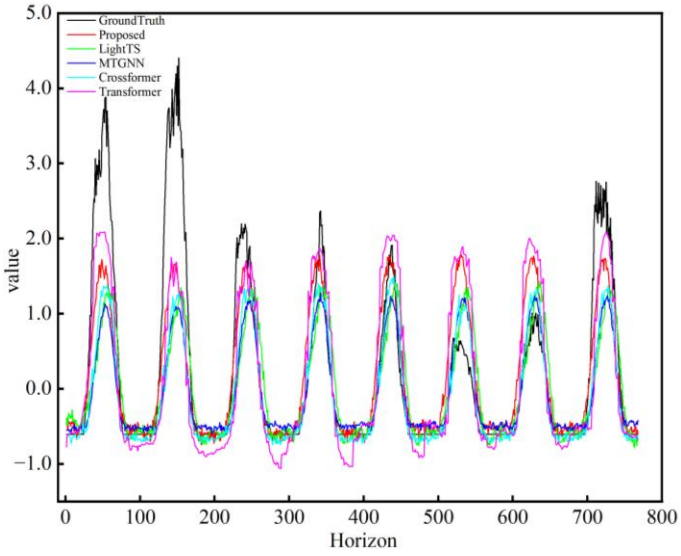

Fig. 5 prediction curves of site 3

5. CONCLUSIONS

In practical scenarios, photovoltaic power generation data is typically collected with environmental information around the photovoltaic power station. The effective utilization of environmental information can enhance the prediction accuracy. This paper proposes a LightTS model based on graph neural networks for long-term photovoltaic power generation prediction. Graph neural network is used to extract environmental information to enhance the prediction performance of LightTS model.

Experiments were conducted on three datasets collected from different terrain and climate sites. The performance of the model was evaluated using MSE and MAE from Horizon 96 to Horizon 768. The results show that different terrains and climates affect the prediction accuracy of the model and the photovoltaic power generation. However, the proposed model always achieves the accurate prediction at all sites, especially in medium and long-term predictions, indicating that the proposed model can effectively utilize environmental information to improve the prediction accuracy of the model.

6. ACKNOWLEDGEMENT

This work is supported by National Science Foundation of China Excellent Young Overseas Talents Program and The Science and Technology Innovation Program of Hunan Province (Ke Yan).

REFERENCE

[1] Al-Shetwi, A. Q., Hannan, M. A., Jern, K. P., Mansur, M., & Mahlia, T. M. I. (2020). Grid-connected renewable energy sources: Review of the recent integration requirements and control methods. *Journal of Cleaner Production*, *253*, 119831.

[2] Yang, D., Li, W., Yagli, G. M., & Srinivasan, D. (2021). Operational solar forecasting for grid integration: Standards, challenges, and outlook. *Solar Energy*, *224*, 930-937.

[3] Notton, G., Nivet, M. L., Voyant, C., Paoli, C., Darras, C., Motte, F., & Fouilloy, A. (2018). Intermittent and stochastic character of renewable energy sources: Consequences, cost of intermittence and benefit of forecasting. *Renewable and sustainable energy reviews*, *87*, 96-105.

[4] Liu, X., Liu, Q., Feng, S., Ge, Y., Chen, H., & Chen, C. (2025). Novel model for medium to long term photovoltaic power prediction using interactive feature trend transformer. *Scientific Reports*, *15*(1), 6544.

[5] Zhang, L., Zhu, J., Zhang, D., & Liu, Y. (2023). An incremental photovoltaic power prediction method considering concept drift and privacy protection. *Applied Energy*, *351*, 121919.

[6] Zhang, T., Zhang, Y., Cao, W., Bian, J., Yi, X., Zheng, S., & Li, J. Less Is More: Fast Multivariate Time Series Forecasting with Light Sampling-oriented MLP Structures 2022. *URL https://arxiv. org/abs/2207.01186*.

[7] Massaoudi, M., Abu-Rub, H., Refaat, S. S., Chihi, I., & Oueslati, F. S. (2021). Deep learning in smart grid technology: A review of recent advancements and future prospects. *IEEE Access*, *9*, 54558-54578.

[8] Qu, Y., Xu, J., Sun, Y., & Liu, D. (2021). A temporal distributed hybrid deep learning model for day-ahead distributed PV power forecasting. *Applied Energy*, *304*, 117704.

[9] Chen, Y., & Xu, J. (2022). Solar and wind power data from the Chinese state grid renewable energy generation forecasting competition. *Scientific data*, *9*(1), 577.

[10] Wu, Z., Pan, S., Long, G., Jiang, J., Chang, X., & Zhang, C. (2020, August). Connecting the dots: Multivariate time series forecasting with graph neural networks. In *Proceedings of the 26th ACM SIGKDD international conference on knowledge discovery & data mining* (pp. 753-763).

[11] Zeng, A., Chen, M., Zhang, L., & Xu, Q. (2023, June). Are transformers effective for time series forecasting?. In *Proceedings of the AAAI conference on artificial intelligence* (Vol. 37, No. 9, pp. 11121-11128).

[12] Vaswani, A., Shazeer, N., Parmar, N., Uszkoreit, J., Jones, L., Gomez, A. N., ... & Polosukhin, I. (2017). Attention is all you need. *Advances in neural information processing systems*,*30*.

[13] Wu, H., Xu, J., Wang, J., & Long, M. (2021). Autoformer: Decomposition transformers with auto-

correlation for long-term series forecasting. *Advances in neural information processing systems*, *34*, 22419-22430.
[14] Zhang, Y., & Yan, J. (2023, May). Crossformer: Transformer utilizing cross-dimension dependency for multivariate time series forecasting. In *The eleventh international conference on learning representations*.
[15] Zhou, H., Zhang, S., Peng, J., Zhang, S., Li, J., Xiong, H., & Zhang, W. (2021, May). Informer: Beyond efficient transformer for long sequence time-series forecasting. In *Proceedings of the AAAI conference on artificial intelligence* (Vol. 35, No. 12, pp. 11106-11115).